

### Quarkonium production at $p\bar{p}$ colliders

V. Barger and A. D. Martin\*

Physics Department, University of Wisconsin, Madison, Wisconsin 53706

(Received 14 November 1984)

We evaluate cross sections for  $\eta(^1S_0)$  and  $\psi(^3S_1)$  quarkonium states of  $c\bar{c}$ ,  $b\bar{b}$ , and  $t\bar{t}$  from lowest-order  $gg \rightarrow \eta, \chi_{0,2}(^3P_{0,2})$  and  $gg \rightarrow \psi g$  subprocesses, including  $\chi_J \rightarrow \psi\gamma$  decays. Data on  $pp$  production of  $\psi$  and  $\Upsilon$  are well described. High rates are predicted for  $\eta_b$  and  $\Upsilon_b$  production at  $p\bar{p}$  colliders. The much smaller  $\eta(t\bar{t})$  and  $\psi(t\bar{t})$  rates are critically dependent on the singular part of the confining potential.

The importance of hadroproduction searches for bound heavy-flavor states  $\mathcal{O}(Q\bar{Q})$  has been dramatically demonstrated in the past by the discoveries of the  $J/\psi$  charmonium and the  $\Upsilon$   $b$ -quarkonium states in  $pp$  collisions. With higher-energy beams now available at  $p\bar{p}$  colliders, it is pertinent to investigate the expected production rates for  $c\bar{c}$  and  $b\bar{b}$  bound states and to estimate whether  $t\bar{t}$  bound states are likely to be produced with sufficiently large cross sections to be detected in forthcoming  $p\bar{p}$  collider experiments. To address these issues we calculate quarkonium ( $\mathcal{O}$ ) production from leading-order QCD subprocesses ( $gg \rightarrow \mathcal{O}$  and  $gg, g\bar{g} \rightarrow \mathcal{O}g$ ) using  $\mathcal{O}$  wave functions at the origin obtained from nonrelativistic potential models. These calculations approximately reproduce the available data on  $pp, p\bar{p} \rightarrow \psi, \chi_c,$  and  $\Upsilon$  cross sections. Encouraged by this success, we make projections for quarkonium production at  $p\bar{p}$  collider energies.

Previous QCD studies of  $\psi$  and  $\Upsilon$  hadroproduction<sup>1</sup> at low transverse momenta were based on semilocal-duality arguments.<sup>2</sup> The cross section from  $gg, q\bar{q} \rightarrow Q\bar{Q}$  subprocesses integrated between  $2m_Q$  and the  $2M(Q\bar{Q})$  threshold was attributed to quarkonium production. Allowing for soft-gluon color rearrangements, a fraction of this cross section gives the vector quarkonium state. This calculation successfully described  $d\sigma/dy(y=0)$ -versus- $M/\sqrt{s}$  and  $d\sigma/dx_F$ -versus- $x_F$  distributions of  $\psi$  and  $\Upsilon$  hadroproduction data up to  $\sqrt{s} = 63$  GeV. The fraction of vector states was found to be strongly dependent on the quarkonium mass, so this duality approach does not lead to definite predictions for  $\mathcal{O}(t\bar{t})$  production at  $p\bar{p}$  collider energies. Also, duality arguments do not specify the relative abundance of the various quarkonium states, such as  $\eta_c:\psi$  and  $\eta_b:\Upsilon$ .

An alternative perturbative QCD approach is to use quarkonia wave functions from a nonrelativistic potential model.<sup>3</sup> The absolute cross sections for individual quarkonium states are then determined. This approach has been used previously<sup>4,5</sup> to explain data on  $\psi$  and  $\Upsilon$  production at high transverse momenta. For our present application to quarkonium cross sections integrated over  $p_T$  we consider the contributions from the lowest-order  $\alpha_s^2$  or  $\alpha_s^3$  diagrams shown in Fig. 1. Other contributions of order  $\alpha_s^3$  with divergent behavior at  $p_T=0$  would be included as nonscaling effects in the initial parton distributions

according to the factorization theorem, and by a semiempirical multiplicative  $K$  factor of order 2 analogous to that needed to account for electroweak  $W^\pm$  and  $Z$  production rates. In our analysis we neglect the small contribution from  $gg \rightarrow \chi_{1g}$ , which may further enhance  $\psi$  production via  $\chi_{1g} \rightarrow \psi\gamma$ .

The leading-order subprocess of Fig. 1(a) for  $\eta, \chi_0,$  or  $\chi_2$  production has the cross section (see, for example, Ref. 6)

$$\hat{\sigma}(gg \rightarrow \mathcal{O}) = \frac{(2J+1)\pi^2}{8M^3} \Gamma(\mathcal{O} \rightarrow gg) \delta \left[ \frac{\hat{s}}{M^2} - 1 \right], \quad (1)$$

where  $M$  is the quarkonium mass,  $J$  is its spin, and the widths in lowest order<sup>7</sup> are given in terms of wave functions evaluated at the origin by

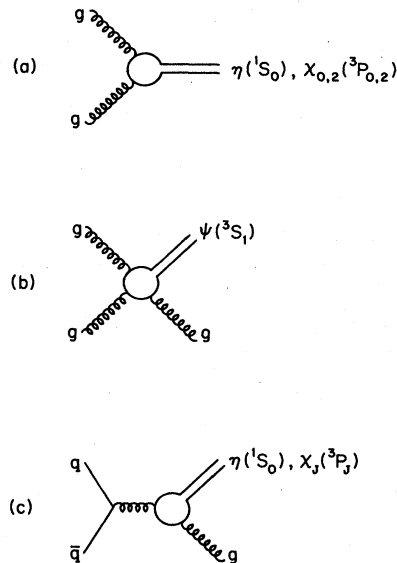


FIG. 1. Lowest-order QCD diagrams for quarkonium hadroproduction.

TABLE I. Partial widths and radiative branching fractions for quarkonium decays calculated using the Wisconsin (Cornell) quarkonium potential. The  $c\bar{c}$   $\chi_J \rightarrow \psi\gamma$  branching fractions are taken from the Particle Data Group tables [Rev. Mod. Phys. 56, S1 (1984)]. To calculate  $B(\chi_J \rightarrow {}^3S_1\psi)$  for  $t$ -quarkonium we have taken the partial width for  $\chi$  single-quark decay to be 47 keV (Ref. 19).

	$\Gamma(\eta \rightarrow gg)$ (MeV)	$\Gamma(\chi_2 \rightarrow gg)$ (MeV)	$B(\chi_2 \rightarrow {}^3S_1\gamma)$ (%)	$B(\chi_0 \rightarrow {}^3S_1\gamma)$ (%)
$c\bar{c}$	18 (18)	1.2 (1.2)	15.5	4.3
$b\bar{b}$	6 (12)	0.14 (0.14)	20 (20)	5 (5)
$t\bar{t}$	2 (26)	0.004 (0.05)	33 (64)	29 (42)

$$\begin{aligned} \Gamma(\eta \rightarrow 2g) &= \frac{8}{3} \alpha_s^2 |R_S(0)|^2 / M^2, \\ \Gamma(\chi_2 \rightarrow 2g) &= \frac{4}{15} \Gamma(\chi_0 \rightarrow 2g) \\ &= \frac{128}{5} \alpha_s^2 |R'_P(0)|^2 / M^4, \end{aligned} \quad (2)$$

where

$$\alpha_s = 12\pi / 25 \ln(M^2 / \Lambda^2);$$

we choose  $\Lambda = 0.2$  GeV. Table I lists widths obtained from the wave functions of two representative potentials that describe  $\psi$  and  $\Upsilon$  mass spectra. The more singular  $r^{-1}$  Cornell potential<sup>8</sup> gives larger widths at high  $M$  than the  $(r \ln r)^{-1}$  singular behavior of the Wisconsin potential<sup>9</sup> that takes into account the  $Q^2$  dependence of  $\alpha_s$ . For the Cornell potential,  $V_c(r) = -\kappa/r + ar$ , we use the parameter choice<sup>10</sup>  $\kappa = 0.494$  and  $a = 0.173$  GeV<sup>2</sup>.

The hadroproduction cross sections are obtained by folding Eq. (1) with the QCD-evolved gluon distributions evaluated at  $Q^2 = M^2$ . Figure 2 shows the results obtained for the universal cross-section-to-width ratio

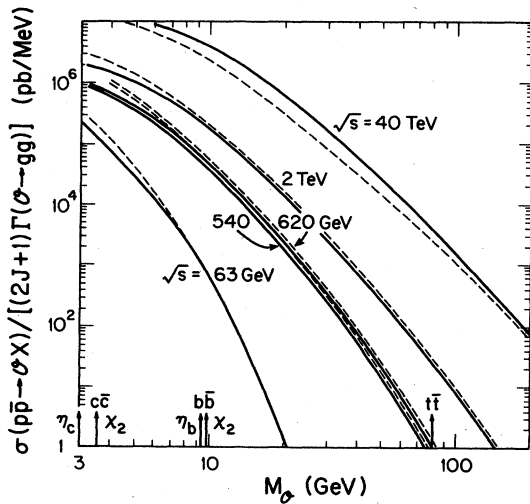


FIG. 2. Universal cross section to width ratio  $\sigma(pp \rightarrow \chi X) / [(2J+1)\Gamma(\chi \rightarrow gg)]$  for gluon-gluon-fusion production (with  $K=1$ ) of heavy-quarkonia states  $\chi(Q\bar{Q})$  versus the quarkonium mass for several c.m. energies  $\sqrt{s}$ . Solid (dashed) curves are obtained with Duke-Owens (Eichten *et al.*) structure functions.

$$\begin{aligned} & \frac{\sigma(pp \rightarrow gg \rightarrow \chi)}{(2J+1)\Gamma(\chi \rightarrow gg)K} \\ &= \frac{\pi^2}{8M^3} \tau \int_{\tau}^1 \frac{dx}{x} D_g(x, Q^2) D_g\left[\frac{\tau}{x}, Q^2\right], \end{aligned} \quad (3)$$

where  $\tau = M^2/s$  and  $D_g$  is the gluon distribution in a proton and  $K$  is a QCD-motivated enhancement factor. For our numerical evaluations we used two recent sets of structure functions, namely, the parametrizations of Duke and Owens<sup>11</sup> and Eichten, Hinchliffe, Lane, and Quigg<sup>12</sup> with  $\Lambda = 0.2$  GeV. These structure functions give significantly differing results only at low  $M/\sqrt{s}$  as shown by the two sets of curves in Fig. 2. For quarkonium hadronic widths that are measured the  $pp$  or  $p\bar{p}$  production cross sections can be directly read off from Fig. 2.

One source of the  ${}^3S_1$  states  $\psi(c\bar{c})$ ,  $\Upsilon(b\bar{b})$ ,  $\psi(t\bar{t})$ , collectively denoted by  $\psi(Q\bar{Q})$ , is  $\chi_J(Q\bar{Q}) \rightarrow \psi(Q\bar{Q})\gamma$  decays. The  $\chi_{0,2}(c\bar{c}) \rightarrow \psi\gamma$  and  $\chi_2(b\bar{b}) \rightarrow \Upsilon\gamma$  branching fractions have been measured. For the other transitions we use potential-model calculations of the partial width as expressed by

$$\Gamma(\chi_J \rightarrow \psi\gamma) = \left(\frac{4}{9}\right) \alpha e_Q^2 k_\gamma^3 |\langle R_S | r | R_P \rangle|^2. \quad (4)$$

For  $t\bar{t}$  the photon momentum  $k_\gamma$  is calculated from the  $\chi_J$  and  $\psi_t$  masses obtained from the potential models with  $m_t = 40$  GeV as input.<sup>13</sup> The branching fractions are summarized in Table I.

The lowest-order direct production of  $\psi(Q\bar{Q})$  states occurs via the so-called bleaching-gluon  $\alpha_s^3$  subprocess<sup>3</sup> of Fig. 1(b), whose cross section is given in terms of the  $\psi \rightarrow 3g$  width

$$\Gamma(\psi \rightarrow 3g) = \frac{40(\pi^2 - 9)\alpha_s^3(M) |R_S(0)|^2}{81\pi M^2} \quad (5)$$

by

$$\hat{\sigma}(gg \rightarrow \psi g) = \frac{9\pi^2}{8M^3(\pi^2 - 9)} \Gamma(\psi \rightarrow 3g) I(\hat{s}/M^2), \quad (6)$$

where

$$I(\gamma) = \frac{2}{\gamma^2} \left[ \frac{\gamma+1}{\gamma-1} - \frac{2\gamma \ln \gamma}{(\gamma-1)^2} \right] + \frac{2(\gamma-1)}{\gamma(\gamma+1)^2} + \frac{4 \ln \gamma}{(\gamma+1)^3}. \quad (7)$$

The calculated  $p\bar{p} \rightarrow \psi\chi$  cross section due to the bleaching-gluon mechanism is comparable in size to that of  $\psi$  production via  $\chi \rightarrow \psi\gamma$  decay. The values for  $c\bar{c}$ ,  $b\bar{b}$ , and  $t\bar{t}$   $\psi({}^3S_1)$  production are given in Table II for two

TABLE II. The cross sections (in nb) for  $\psi({}^3S_1)$  production via  $gg \rightarrow \psi g$  and  $\chi_J \rightarrow \psi\gamma$ , respectively at  $\sqrt{s} = 63$  GeV (620 GeV). The calculations are based on the Wisconsin quarkonium potential. For the Cornell potential, the  $t\bar{t}$  cross sections would be an order of magnitude larger.

	$c\bar{c}$	$b\bar{b}$	$t\bar{t}$
$\sigma(pp \rightarrow gg \rightarrow \psi g)$	280 (3000)	0.13 (19)	$(3 \times 10^{-5})$
$\sigma(p\bar{p} \rightarrow gg \rightarrow \chi_J \rightarrow \psi\gamma)$	300 (1800)	0.24 (15)	$(2.5 \times 10^{-5})$

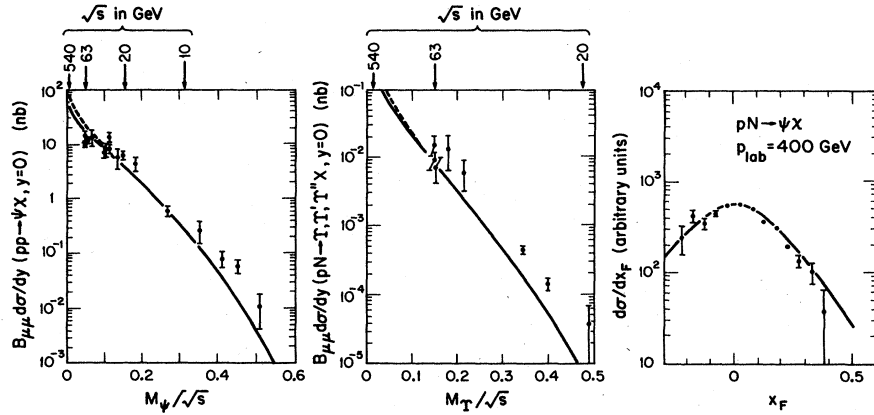


FIG. 3. Comparison of  $gg \rightarrow \chi \rightarrow \psi(Q\bar{Q})\gamma$  and  $gg \rightarrow \psi(Q\bar{Q})g$  model predictions with data on  $\psi(3.1)$  and  $\Upsilon(9.46)$  production (a), (b)  $d\sigma/dy$  at  $y=0$  versus  $\sqrt{s}$ , (c)  $d\sigma/dx_F$  versus  $x_F$ . Leptonic branching fractions  $B(\psi \rightarrow \mu\bar{\mu})=0.074$  and  $B(\Upsilon \rightarrow \mu\bar{\mu})=0.03$  are used. Data are from Ref. 14.

typical energies,  $\sqrt{s}=63$  and  $620$  GeV. For  $c\bar{c}$  at  $\sqrt{s}=63$  GeV the bleaching-gluon and  $\chi$ -decay contributions are about equal in accord with experiment.<sup>14</sup>

An additional bleaching-gluon contribution originates from  $q\bar{q}$  fusion [Fig. 1(c)]. The threshold divergence in  $q\bar{q} \rightarrow \chi_{Jg}$  at  $s=M^2$  (equivalent to the singularity in  $\chi_J \rightarrow q\bar{q}g$  decays) is due to the breakdown of the nonrelativistic model for quarkonium states and can be regularized by requiring  $(\hat{s})^{1/2} > M + \Delta$  with  $\Delta \sim 0.3$  GeV. However, the  $\eta$  and  $\psi$  (from  $\chi \rightarrow \psi\gamma$ ) cross sections obtained from  $q\bar{q} \rightarrow \mathcal{O}g$  were found to be insignificant in comparison with the  $gg$  initiated subprocesses. As a consequence the quarkonium production rates in  $pp$  and  $p\bar{p}$  collisions should be equal, which is compatible with the available  $\psi(3.1)$  production data<sup>15</sup> at accelerator energies.

This model for vector-quarkonium production is compared with data on  $\psi(3.1)$  and  $\Upsilon(9.8)$  production<sup>14-16</sup> in Fig. 3, taking  $K=2$ . The normalization of the cross section, the  $M/\sqrt{s}$  dependence of  $d\sigma/dy$  at  $y=0$ , and the shape of the  $x_F$  distribution are reasonably well reproduced ( $\Upsilon', \Upsilon''$  contributions are not included in the calculation). The  $y$  and  $x_F$  variables are defined as in Ref. 1.

The predicted energy dependence of the  $\eta$  and  $\psi$  quarkonium cross sections are given in Fig. 4. The following statements can be made about the results.

(i) For any hidden flavor,  $\eta$  production is larger than  $\psi$  by about an order of magnitude (see also Ref. 4).

(ii) With the present CERN  $p\bar{p}$  collider integrated luminosity of approximately  $100 \text{ nb}^{-1}$  at  $\sqrt{s}=540$  GeV about 100 000  $\eta_b$  would have been produced. The rare decay mode  $\eta_b \rightarrow \gamma\gamma$ , with branching fraction of order 0.1% or less, or the expected  $\eta_b \rightarrow \Lambda\bar{\Lambda}$  mode may provide a possible means to search for the  $\eta_b$  in  $p\bar{p}$  data.

(iii) An  $\Upsilon$  cross section of about 30 nb is predicted at  $\sqrt{s}=540$  GeV and so the existing data sample should contain about 100  $\Upsilon \rightarrow \mu^+\mu^-$  events. Detection of these requires muon identification down to transverse momentum of  $p_T \approx 5$  GeV.

(iv) Enormous numbers of  $\eta_c$  and  $\psi(c\bar{c})$  events are produced at  $p\bar{p}$  collider energies but only those at high  $p_T$  are likely to be detected.<sup>4,5</sup>

(v) The predictions for  $\mathcal{O}(t\bar{t})$  production depend very sensitively on the singular part of the potential, with larger cross sections expected for a  $1/r$  behavior at small  $r$ .  $t$ -quarkonium detection will be difficult at collider energies up to  $\sqrt{s}=2$  TeV. The higher-cross-sections predictions in Fig. 4 at 2 TeV are  $\sigma(\eta_t) \sim 1$  nb and  $\sigma(\psi_t) \sim 20$  pb. The expected branching fractions<sup>4,17</sup>  $B(\eta_t \rightarrow \gamma\gamma) \sim 0.2\%$  and  $B(\psi_t \rightarrow \mu^+\mu^-) \sim 3\%$  suppress these detectable modes.

(vi) If a light Higgs boson exists, the radiative decay<sup>18</sup>  $\psi_t \rightarrow H\gamma$  provides a good  $t$ -quarkonium signature of a high- $p_T$  photon. In the standard model  $B(\psi_t(80) \rightarrow H\gamma) \lesssim 1\%$ .

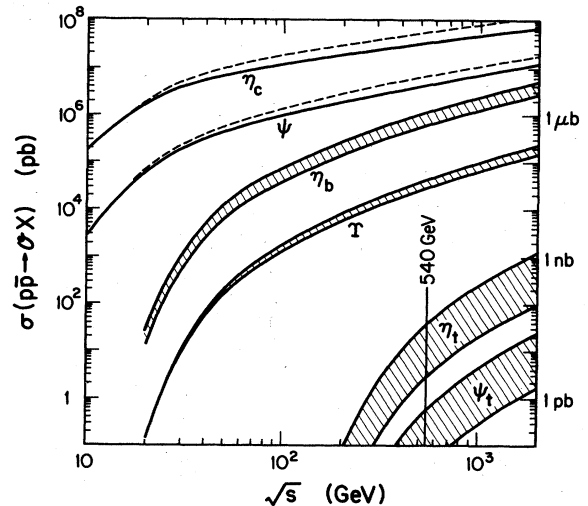


FIG. 4. Predicted cross sections with  $K=2$  for heavy-quark bound states, resulting from  $gg \rightarrow \eta, \chi_{0,2}$  and  $gg \rightarrow \psi g$  production with  $\chi_{0,2} \rightarrow \psi\gamma$  decays, versus the c.m. energy  $\sqrt{s}$ . The shaded regions for production of  $b\bar{b}$  and  $t\bar{t}$  (80 GeV) states are representative of the uncertainty in potential model calculations; the lower (higher) curves correspond to the Wisconsin (Cornell) potential (Refs. 8–10). Solid (dashed) curves correspond to use of Duke-Owens (Eichten *et al.*) structure functions.

## ACKNOWLEDGMENTS

We thank K. Hagiwara, W. F. Long, and M. G. Olsson for useful discussions and S. Jacobs for performing potential model calculations. This research was supported in

part by the University of Wisconsin Research Committee with funds granted by the Wisconsin Alumni Research Foundation, in part by the Department of Energy under Contract No. DE-AC02-76ER00881, and by the U. K. Science and Engineering Research Council.

\*Permanent address: University of Durham, Physics Department, Durham, England.

<sup>1</sup>V. Barger, W. Y. Keung, and R. J. N. Phillips, *Z. Phys. C* **6**, 169 (1980).

<sup>2</sup>H. Fritzsch, *Phys. Lett.* **67B**, 217 (1977).

<sup>3</sup>W.-Y. Keung, in *Proceedings of the Z<sup>0</sup> Physics Workshop, Ithaca, New York, 1981*, edited by M. E. Peskin and S.-H. Tye (Cornell University Report No. 81-485, 1981); E. L. Berger and D. Jones, *Phys. Rev. D* **23**, 1521 (1981); L. Clavelli, P. H. Cox, and B. Harms, *ibid.* **29**, 57 (1984).

<sup>4</sup>R. Baier and R. Ruckl, *Z. Phys. C* **19**, 251 (1983); *Nucl. Phys. B* **208**, 381 (1982).

<sup>5</sup>F. Halzen, F. Herzog, E. W. N. Glover, and A. D. Martin, *Phys. Rev. D* **30**, 700 (1984).

<sup>6</sup>V. Barger, H. Baer, and K. Hagiwara, *Phys. Rev. Lett.* **53**, 641 (1984).

<sup>7</sup>R. Barbieri, R. Gatto, and R. Kögerler, *Phys. Lett.* **60B**, 1976 (1976).

<sup>8</sup>E. Eichten, *Phys. Rev. Lett.* **34**, 369 (1975); E. Eichten and K. Gottfried, *Phys. Lett.* **66B**, 286 (1977); E. Eichten, K. Gottfried, T. Kinoshita, K. D. Lane, and T. M. Yan, *Phys. Rev. D* **21**, 203 (1980).

<sup>9</sup>K. Hagiwara, S. Jacobs, M. G. Olsson, and K. J. Miller, *Phys. Lett.* **131B**, 455 (1983).

<sup>10</sup>K. J. Miller and M. G. Olsson, *Phys. Rev. D* **25**, 2383 (1982).

<sup>11</sup>D. Duke and J. Owens, *Phys. Rev. D* **30**, 49 (1984).

<sup>12</sup>E. Eichten, I. Hinchliffe, K. Lane, and C. Quigg, *Rev. Mod. Phys.* **56**, 579 (1984).

<sup>13</sup>UA1 collaboration, C. Rubbia, talk at Neutrino '84 conference, Dortmund, 1984 (unpublished); D. DiBitonto, talk at VIIth European Symposium on Antiproton Interactions, Durham, 1984 (unpublished); V. Barger, A. D. Martin, and R. J. N. Phillips, CERN Report No. TH. 3972, 1984 (unpublished).

<sup>14</sup>C. Kourkouvelis *et al.*, *Phys. Lett.* **81B**, 405 (1979).

<sup>15</sup>K. J. Anderson *et al.*, *Phys. Rev. Lett.* **42**, 944 (1979).

<sup>16</sup>L. Camilleri, in *Proceedings of the 1979 International Symposium on Lepton and Photon Interactions at High Energies, Fermilab*, edited by T. B. W. Kirk and H. D. I. Abarbanel (Fermilab, Batavia, Illinois, 1980); A. L. S. Angelis *et al.*, *Phys. Lett.* **87B**, 398 (1979); J. H. Cobb *et al.*, *ibid.* **68B**, 104 (1977); E. J. Siskind *et al.*, *Phys. Rev. D* **21**, 628 (1980).

<sup>17</sup>J. P. Leveille, in *Proceedings of the Z<sup>0</sup> Physics Workshop, Ithaca, New York, 1981* (Ref. 3), p. 241.

<sup>18</sup>F. Wilczek, *Phys. Rev. Lett.* **39**, 1304 (1977).

<sup>19</sup>J. H. Kuhn and S. Ono, *Z. Phys.* **21**, 395 (1984).